Composite Structures 178 (2017) 372–382

Contents lists available at ScienceDirect

Composite Structures

journal homepage: www.elsevier.com/locate/compstruct

CFRP-ECC hybrid for strengthening of the concrete structures

Chao Wu [a,b], Victor C. Li [b,*]

[a] School of Transportation Science and Engineering, Beihang University, 37 Xueyuan Road, Beijing 100191, China
[b] Department of Civil and Environmental Engineering, University of Michigan, Ann Arbor, MI 48109, USA

ARTICLE INFO

Article history:
Received 25 November 2016
Revised 1 May 2017
Accepted 12 July 2017
Available online 13 July 2017

Keywords:
Carbon fiber reinforced polymer (CFRP)
Engineered cementitious composite (ECC)
Bond
Strengthening
Concrete
Beam

ABSTRACT

The strengthening of concrete structures using FRP composite and polymer adhesive has been challenged considering structural fire. This technology is limited to situations with low fire hazards. Though the cementitious adhesive showed improved fire resistance than the polymer counterpart, the former faces challenges of brittleness and high temperature spalling. This paper proposes a CFRP-ECC hybrid system for strengthening of the concrete structures. This hybrid consists of CFRP composite embedded in the ECC matrix. CFRP functions as the main load-carrying element, while ECC acts as the adhesive layer for protecting the CFRP and transferring the load between the concrete structure and CFRP. ECC is ductile in tension and has been shown to have improved fire performance without spalling over normal cementitious materials. In this paper, ECC was developed with a tensile strain capacity of 3%. Then direct pull-out tests were conducted to quantify the interface behavior between CFRP and ECC, and to obtain the effective bond length of CFRP. Finally a concrete beam with the CFRP-ECC hybrid strengthening was tested under four-point bending. The experimental results showed that the effective bond length of CFRP in ECC was longer than 170 mm. When the CFRP-ECC hybrid was used for strengthening of the concrete beam, premature debonding occurred at the interface between CFRP-ECC hybrid layer and the surface of the concrete beam, thus the flexural behavior of the concrete beam was barely improved. Therefore, it is recommended that proper surface treatment of the concrete beam should be prepared or innovative anchoring techniques should be developed before the CFRP-ECC hybrid can be used for the strengthening of the concrete structures.

1. Introduction

There has been a considerable increase in the demand of repair and strengthening of the concrete structures worldwide [1–3]. With high strength to weight ratio and desirable resistance to the harsh environment, fiber reinforced polymer (FRP) composites have been widely accepted for the strengthening of the concrete structures [1–8]. Polymer adhesives, like epoxy, are normally adopted as the bonding agent [9–11]. One major issue with the polymer adhesives is that, when the glass transition temperature (T_g) is exceeded, the mechanical properties of the adhesive is reduced and the strengthening effect of the FRP cannot be maintained [12–17]. Unfortunately, most of the polymer adhesives used for the structural strengthening have a T_g less than 100 °C [18]. A study in [19] found that the efficiency of the CFRP strengthening of the concrete structures would extensively reduce by 65% at 300 °C [20].

In order to solve this problem, cement based adhesives are introduced for the FRP strengthening of the concrete structures [12,21–23]. Although the bond behavior between the FRP and the concrete is improved under the elevated temperatures, another problem of the cement based adhesives has been observed [21,24,25]. Since most of the cement based adhesives lack ductility, the load cannot be effectively transferred from the concrete to the FRP composite. Also the failure is generally brittle and lack warning [21]. It was found that the FRP-mortar system was generally less effective than the FRP-epoxy system in strengthening. For example, it was concluded that the FRP-mortar system was 45% [26] and 50% [27] less effective than the FRP-epoxy counterparts.

Therefore, it is necessary to develop a cementitious adhesive with desired ductility, which can effectively distribute and transfer the load from the concrete substrate to the FRP composite, without deterioration under elevated temperatures. Engineered Cementitious Composites (ECC) is a promising candidate for such strengthening applications [28,29]. ECC was developed based on the micro fracture mechanics with a strain capacity in the range of 3–7% [30], comparing to 0.1% for ordinary Portland cement (OPC) mortar. This

* Corresponding author.
E-mail addresses: wuchao@buaa.edu.cn (C. Wu), vcli@umich.edu (V.C. Li).

http://dx.doi.org/10.1016/j.compstruct.2017.07.034
0263-8223/

ductility of ECC is achieved by micro-cracking (with micro-crack width less than 100 μm [30]) in the strain hardening stage [31]. More importantly, ECC can effectively resist spalling failure under elevated temperatures up to 800 °C, due to the melting of PVA fibers [32].

Considering these advantages, ECC has great potential as adhesive for the FRP strengthening of the concrete structures [33–35]. In a recent study [33], ECC was used as the adhesive for bonding the basalt fiber reinforced polymer (BFRP) grid to the concrete beams for the flexural strengthening. Uniform tiny cracks were observed in ECC during the loading process, and the load carrying capacity of the concrete beam was increased by 35% maximum. The authors of this paper investigated the CFRP-ECC hybrid behavior under elevated temperatures up to 500 °C [35]. It was found that ECC showed desirable anti-spalling behavior with the temperature up to 500 °C. The compression and tensile strengths of ECC showed little reduction with the temperature up to 300 °C. It was found that the interface between ECC and the concrete substrate was sensitive to the temperature, and premature failure may occur at the interface during the pull-out tests of CFRP. However, the existing studies on the FRP-ECC hybrid for the strengthening of the concrete structures only focused on the failure mechanism and the improvement in the load-carrying capacity of the concrete beams. Very few work reported the comprehensive characterization of the ECC material, and fundamental investigation on the CFRP-ECC interface behavior (e.g. effective bond length).

As part of a project on the development of the CFRP-ECC hybrid for the strengthening of the concrete structures, this paper presents comprehensive experimental results of this hybrid under room temperature. The thermal-mechanical behavior of this hybrid under elevated temperatures has been reported in [35]. This paper firstly focused on the development of ECC as the adhesive for the CFRP strengthening. Then the interface behavior between CFRP and ECC was investigated through direct pull-out tests. Various CFRP bond lengths were used in the pull-out tests in order to find out the effective bond length of the CFRP-ECC hybrid. Finally, four-point bending tests were conducted on steel reinforced concrete beams strengthened with the CFRP-ECC hybrid. The failure modes and the load-displacement responses were reported. For comparison purpose, the corresponding mortar specimens were also prepared and tested under the same condition as ECC specimens in all tests. The advantages of ECC as the adhesive comparing to the cement mortar were discussed. This paper contributes to the fundamental understanding on the interface behavior between CFRP and ECC, and provides comprehensive experimental data and necessary precautions for the future design of the CFRP-ECC hybrid for the strengthening of the concrete structures.

2. Experimental program

The proposed method using the CFRP-ECC hybrid for the strengthening of the concrete structures are tested with an experimental program of three steps. Firstly, ECC was developed and the material properties were characterized through compressive and tensile tests. Then direct pull-out tests were conducted to study the interface behavior between CFRP and ECC. Finally, four-point bending tests were carried out on the steel reinforced concrete beams to investigate the strengthening effect of the CFRP-ECC hybrid system. The three testing steps will be described respectively in the following sections.

2.1. Compression and tension tests of ECC

The mixture proportion of ECC used in the current study is presented in Table 1. The major matrix ingredients of ECC include Type I ordinary Portland cement, Class F fly ash, fine aggregate (F-75 silica sand), water and water reducer (ADVA-190). The fly ash was provided by the DTE Monroe Power Plant in the State of Michigan. The chemical properties of the fly ash provided by the manufacturer are listed in Table 2. The F-75 silica sand has a maximum and an average grain size of 250 μm and 110 μm, respectively. The Poly-Vinyl Alcohol (PVA) fibers are 12 mm long with a diameter of 39 μm. The PVA fibers are coated with 1.2% by weight of oil to control the fiber/matrix interfacial properties. The volume content of the PVA fiber in ECC was 2%. The detailed information of the PVA fiber has been well documented in the publications by the ACE-MRL group at the University of Michigan [32] as summarized in Table 3.

The ECC mixture was prepared in a Hobart type mixer of 10 L capacity. Firstly, cement, sand and fly ash were dry mixed for 5 min at the low speed of the mixer. Then the mixture of water and water reducer was added and mixed for another 4 min under the same speed. Then the mixture was checked and the blocks were broken to ensure a homogeneous paste status. The mixing continued for another 2 min until the paste reached a good fluidity. Then the PVA fibers were added slowly into the mortar and mixed for 5 min under the medium speed of the mixer. Then the mixture was checked and the glomeration of the fibers was broken to ensure a uniform dispersion of the fibers. Finally, the mixing continued for another 3 min until the fibers were well dispersed.

The fresh ECC was cast into the molds that were moderately vibrated using a vibration table. The molds were sealed with plastic bags and subsequently demolded after 1 day curing. All specimens were cured for another 27 days in air (23 ± 3 °C; 30 ± 10% RH) before testing. Both cube specimens and dogbone-shaped specimens were prepared for compressive and tensile testing respectively. The cube specimens had a dimension of $50 \times 50 \times 50\ mm^3$ according to ASTM C190/C190M [38]. The dimensions of the dogbone-shaped specimens can be found in [39], which were recommended by the Japan Society of Civil Engineers (JSCE) [40] for standardized tensile testing of ECC.

The compression tests were conducted on a FORNEY F-50F-F96 machine under load control at a speed of 20 MPa/min. The peak load was recorded to determine the compressive strength. The tension tests were carried out on a servo-hydraulic Instron 5969 testing system with a capacity of 50 kN, using displacement control at a speed of 0.5 mm/min. The experimental setup of the tensile testing is presented in Fig. 1. Two linear variable displacement transducers (LVDT), with a gauge length of approximately 100 mm, were attached to the specimen. Stress-strain curves were then recorded to determine the behavior of the specimens under direct tension.

For comparison purpose, mortar cube and dogbone specimens (ECC without PVA fibers) were also prepared. The mix proportion, preparation process and testing setup were all the same as ECC specimens except that mortar specimens were without PVA fibers.

2.2. Pull-out test of CFRP-ECC hybrid system

Direct pull-out tests were conducted in order to investigate the interface behavior between CFRP and ECC of the hybrid system. Since this system was proposed for the strengthening of the concrete structures, a concrete block was also included when preparing the pull-out specimen. The experimental setup and dimensions of the specimen are presented in Fig. 2. The specimen seated on a steel base plate and was secured in position by the top steel plate which was fastened to the base plate through two steel rods. A stopper was mounted on the base plate to prevent any lateral movement of the specimen during the loading process. The stopper can also be adjusted when installing the specimen so that the CFRP sheet was in the vertical direction. A spirit level was used to check the straightness of the CFRP sheet before testing. The CFRP sheet

Table 1
Mixture proportion of ECC in the current study (kg/m^3).

Water (W)	Cement (C)	Fly ash (FA)	Silica sand	PVA fiber	Water reducer	W/(C + FA)	FA/C
311	393	865	457	26	5	0.25	2.20

Table 2
Chemical composition and physical properties of fly ash provided by manufacturer.

Chemical composition, %	Fly ash
CaO	15.66
SiO_2	42.20
Al_2O_3	22.51
Fe_2O_3	9.20
SO_3	1.85
MgO	3.20
Na_2O	0.98
K_2O	1.53
Moisture	0.12
Loss on ignition	1.34
Physical properties	
Fineness,% retained on #325	16.58
Water requirement,%	95
Density	2.53

was 50 mm wide and was embedded in the middle of the ECC layer which was attached to the concrete block. Two LVDTs were used to record the relative movement between the CFRP sheet and the ECC. The LVDTs were the same as those in Fig. 1. The gauge length of each specimen was recorded and used for the calculation of the relative slip between CFRP and ECC (see the detailed discussions in Section 3.2).

CFRP sheet was Tyfo SCH-41 provided by MTC Corporation in St. Louis with a measured thickness of 0.55 mm. The tensile tests were conducted according to the ASTM D3039 [41]. The tensile strength was not achieved due to the difficulty of clamping the CFRP sheets. The tested modulus was 79.7 GPa with the applied stress up to 833.5 MPa. Six repeating tests were conducted to measure this modulus. The nominal tensile strength of CFRP sheet was 986 MPa. The mixture proportion of ECC was the same as that in Table 1. The concrete mixture is presented in Table 4. The compression strength of the concrete was tested using a concrete cylinder of 75 mm in diameter according to ASTM C873/C873M [42]. The 28-day compressive strength was 40.5 MPa.

The preparation procedure of the pull-out specimens is presented in Fig. 3. Firstly, the surface of the concrete block was prepared after 28 days of curing. The cement on the surface was removed and the course aggregates were exposed. The purpose of the surface treatment was to ensure the bonding quality between ECC and concrete, so that this interface would not be a problem during the pull-out tests. Then the concrete blocks were placed in a mold, where the CFRP sheets can be secured in position. The first layer of the fresh ECC of 12.5 mm thick was applied on top of the concrete block and underneath the CFRP sheet. Finally another layer of ECC of 12.5 mm thick was casted on top of the CFRP sheet. The thickness of the ECC layer was 25 mm with the CFRP sheet embedded in the middle. The specimens were demolded after 1 day and cured for another 27 days in air (23 ± 3 °C; 30 ± 10% RH). Because the concrete block was cured for 56 days before pull-out tests, its 56-day compressive strength was also tested which was 41.7 MPa (only 3% higher than the 28-day strength which was 40.5 MPa).

In order to study the effect of the embedded length of CFRP on the interface behavior between CFRP and ECC, five embedded lengths were selected as 25 mm, 50 mm, 75 mm, 100 mm, 135 mm and 170 mm. For each embedded length, at least three identical specimens were prepared and tested for repeating purpose. The pull-out tests were conducted on a MTS 810 material testing system with a loading capacity of 100 kN. Displacement control was used at a loading speed of 0.5 mm/min. The pull-out test was continued until the load dropped dramatically or the CFRP sheet was pull out by 30 mm from LVDT reading.

For comparison purpose, the pull-out specimens were also prepared with CFRP embedded in a mortar layer (ECC without PVA fiber, see Table 1). The mixture proportion of the mortar was the same as that of ECC but without PVA fibers. The specimen preparation process and the loading scheme were kept the same as the ECC specimens.

2.3. Four-point bending tests on concrete beams

Three identical steel reinforced concrete beams were prepared. The first beam was used as reference. The second beam was strengthened with CFRP-ECC hybrid system. The third beam was the same as the second beam except that ECC was replaced with mortar (ECC without PVA fiber, see Table 1). The dimensions of the beam and the four-point bending test setup are presented in Fig. 4. The total length of the beam was 1524 mm (60 in) with a span length of 1372 mm (54 in). As can be seen in Fig. 4, the strengthening layer was 1067 mm (42 in) long and was not extended under the supports. This was because in real applications, the concrete beams are normally rigidly connected to the columns, which makes it difficult to extend the strengthening layer into the column.

The longitudinal steel rebar was 12.7 mm (0.5 in) in diameter and the stirrup was 6.4 mm (0.25 in) in diameter. The stirrups had a spacing of 76 mm (3 in). Both rebar and stirrup were Grade 60 according to ASTM A615/A615M [43] with a nominal yielding strength of 469 MPa. The concrete mix proportion was the same as in Table 4. The strengthening layer (25 mm thick) was either CFRP-ECC hybrid or CFRP-mortar hybrid for comparison purpose. The mix proportion of ECC or mortar can be found in Table 1.

Fig. 5 shows the preparation process of the strengthened concrete beam. It should be noted that, the concrete beam was casted in the mold in an upside down position, which made it easier to apply the hybrid strengthening layer. Firstly, the bottom surface of the concrete beam was treated after 28 days curing with the coarse aggregates exposed. This was to ensure a better interface bonding between concrete and ECC. Then a layer of ECC of 12.5 mm thick was applied on the concrete surface. The CFRP sheet of 100 mm was placed on top of the first ECC layer and finally the second layer of ECC of 12.5 mm thick was applied. The CFRP sheet was thus embedded in the middle of ECC layer.

Table 3
Properties of PVA fiber [31–33].

Diameter (μm)	Length (mm)	Nominal strength (MPa)	Modulus (GPa)	Density (kg/m^3)	Melting point (°C)
39	12	1600	42	1300	230

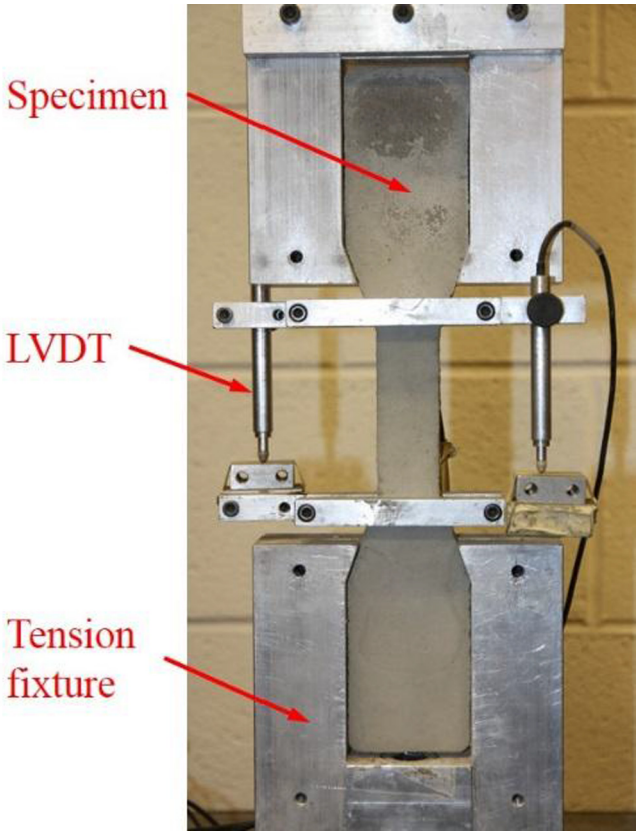

Fig. 1. Experimental setup of tensile testing.

The four-point bending tests were conducted on a servo-hydraulic testing system with a loading capacity of 500 kN. The tests were under displacement control with a loading speed of 1 mm/min. The mid-span displacement was recorded with an optical tracking system, Optotrak Certus, from NDI Measurement Sciences. The experimental setup of the four-point bending tests is shown in Fig. 6.

3. Experimental results and discussions

3.1. Compressive and tensile properties of ECC

For the compressive strength of ECC, six cube specimens were tested and the average compressive strength was 50.9 MPa. The ECC mortar without PVA fiber was also tested and the compressive strength was 52.6 MPa. Five specimens were tested for the tensile properties of ECC and mortar, respectively. The tensile stress-strain curves of ECC at the age of 28 days are plotted in Fig. 7, with a typical multiple-cracking image of ECC. The tensile properties of ECC and mortar are listed in Table 5.

In Table 5, the first crack strength was determined from the point where the stress-strain curve becomes non-linear [40]. Peak stress and the corresponding strain were defined as "tensile strength" and "tensile strain", respectively. In the case when slight stress decrease after the peak stress was observed, the strain at 95% of the peak stress was used as the "tensile strain" [39]. The strain hardening behavior of ECC is obvious in Fig. 7, with the tensile strain almost 252 times higher than that of the mortar (see Table 5).

3.2. Interface behavior of the CFRP-ECC hybrid system

Pull-out tests were conducted to investigate the interface behavior between CFRP and ECC. Various CFRP embedded length were selected as 25 mm, 50 mm, 75 mm, 100 mm, 135 mm and 170 mm. For each embedded length, at least three specimens were tested for repeating purpose. The detailed experimental setup can be found in Section 2.2. The stress versus the relative slip between CFRP and matrix are presented in Fig. 8. The stress, σ, is equal to the applied load, P, divided by the section area of CFRP. The relative slip, δ, can be calculated by the following equation:

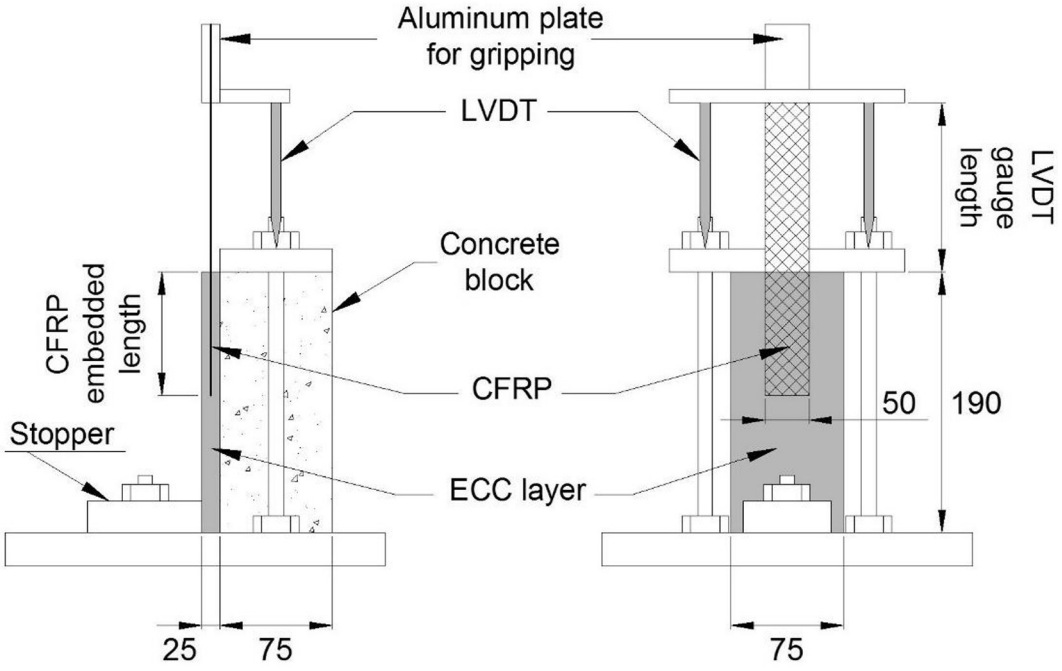

Fig. 2. Experimental setup of pull-out tests and specimen dimensions (unit in mm, not to scale).

Table 4
Mixture proportion of concrete (kg/m^3).

Water	Cement	Stone	Sand
200	476	1105	562

$$\delta = \Delta - \frac{PD}{WtE} \quad (1)$$

where Δ is the LVDT readings; D is the gauge length of LVDT (see Fig. 2); W and t are the width and thickness of CFRP sheet which are 50 mm and 0.55 mm respectively; E is the modulus of CFRP which was measured as 79.7 GPa.

As can be seen in Fig. 8, the ECC and mortar specimens showed similar development of the pull-out stress against the relative slip between CFRP and the matrix (either ECC or mortar). Firstly, the stress increased with the slip up to a peak point after which a fast decrease of the stress was observed. Finally the stress became stabilized at a very low level with the increase of the slip. The last stable stage of the stress was attributed to the friction between CFRP and the matrix. It is obvious in Fig. 8 that the peak stress of ECC specimen seems proportionally increase with the embedded length of CFRP, while it is not the case for the mortar specimens. The peak stress stopped increasing for mortar specimens when the embedded length exceeded 100 mm (Fig. 8b).

The peak stress of each specimen was extracted from the stress-slip curve and plotted against the embedded length in Fig. 9(a) for ECC specimens and in Fig. 9(b) for mortar specimens. In Fig. 9, the symbol represents the average peak stress of repeating specimens and the error bar refers to the standard deviation. It is clear that the pull-out peak stress of ECC specimens increased with the CFRP embedded length. For example, the average peak stress of ECC-25 was 71.6 MPa, and it increased to 174.2 MPa (143.3%) when the embedded length was 170 mm. Similarly, the peak stress of the mortar specimens increased from 37.2 MPa to 154.3 MPa when the CFRP embedded length changed from 25 mm to 100 mm. However, the increasing trend stopped when the CFRP embedded length exceeded 100 mm. For example, the peak strength of Mortar-135 and Mortar-170 was 133.5 MPa and 142.6 MPa, respectively.

The different increasing trends of the peak stress between ECC and mortar specimens can be attributed to their different failure modes. All ECC specimens failed by CFRP being pulled out from ECC (see Fig. 10a). However, two different failure modes were observed for the mortar specimens. When the embedded length was shorter than 100 mm, CFRP was pulled out from the mortar matrix (similar to Fig. 10a). When the embedded length exceeded 100 mm, the mortar layer failed by shear cracking under the tensile loading transferred by the CFRP sheet. Then the CFRP was pulled out from the rest of the mortar layer (see Fig. 10b). The failure modes indicated that the CFRP-mortar hybrid may hardly sustain the load transferred from the CFRP when the embedded length was longer than 100 mm. Therefore, the effective bond length of CFRP with ECC as adhesive may be longer than 170 mm, whereas the effective bond length of CFRP with mortar as adhesive was in the range of 100 mm–135 mm. In a similar study by Hosseini and Mostofinejad [44], CFRP sheet (SikaWrap230C) was bonded to the concrete prism using external bonded reinforcement (EBR) technique using the adhesive of Sikadur 330. Single shear tests were conducted and the corresponding effective bond length was identified as 35 mm. The effective bond length reported by Hosseini and Mostofinejad was based on the conventional EBR technique and was much smaller than the effective bond length of the CFRP-mortar or CFRP-ECC hybrid in the current study.

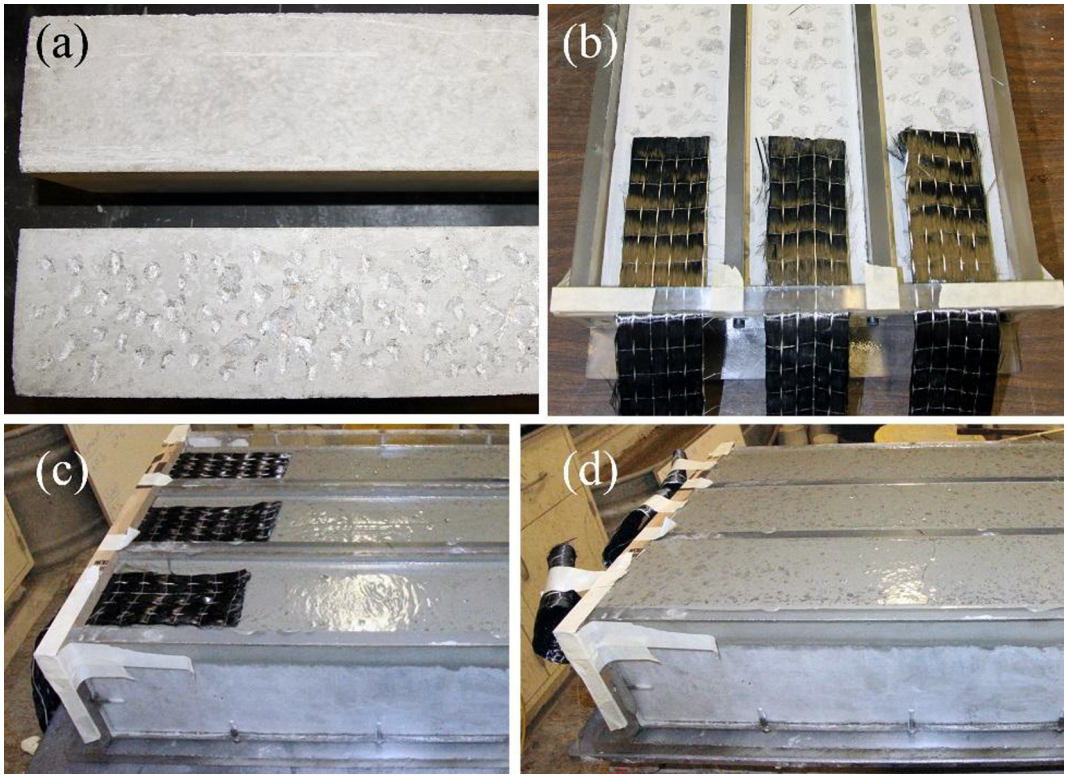

Fig. 3. Preparation process of pull-out specimens: (a) surface treatment of concrete block; (b) CFRP sheet positioning; (c) apply the first layer of ECC and (d) apply the second layer of ECC.

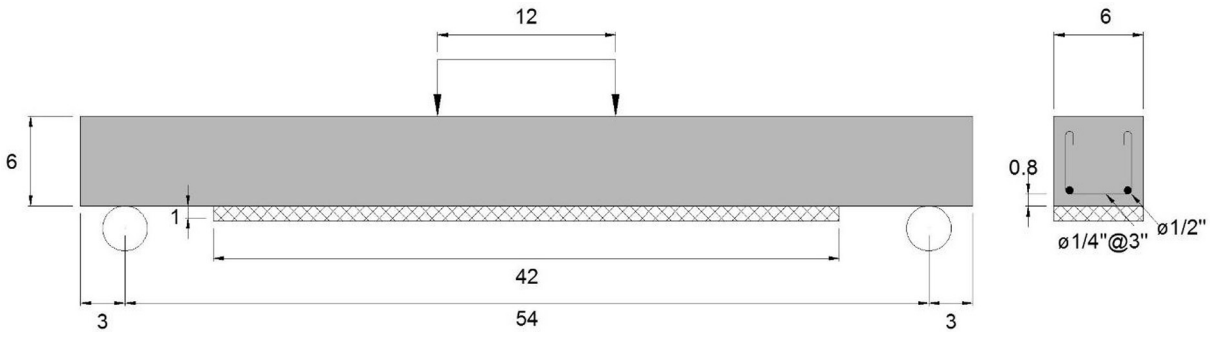

Fig. 4. Dimensions of strengthened concrete beam and four-point bending setup (unit in inch).

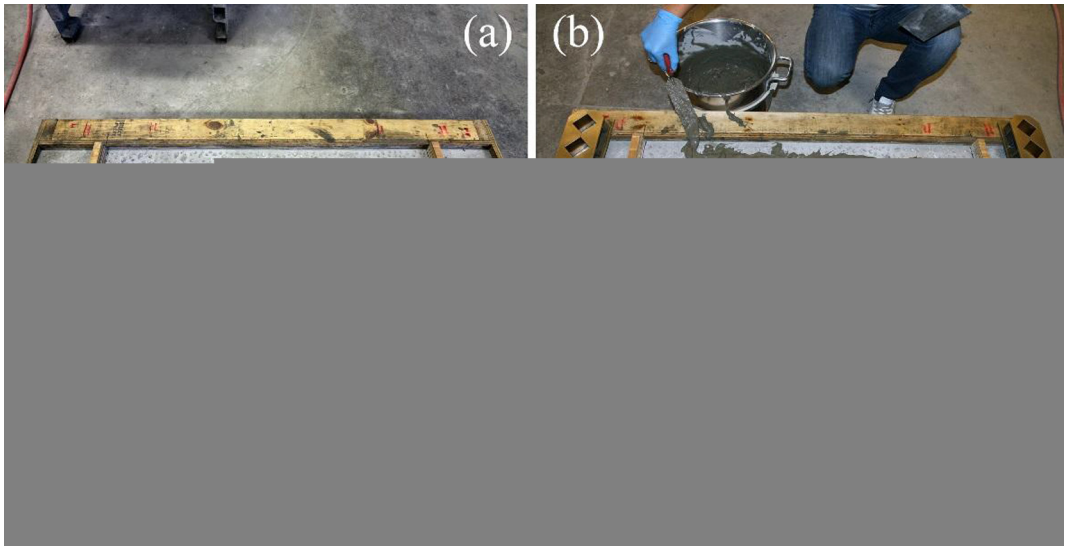

Fig. 5. Preparation process of the concrete beam with CFRP-ECC hybrid strengthening: (a) bottom surface treatment of the concrete beam; (b) apply the first layer of ECC; (c) apply CFRP sheet; (d) apply the second layer of ECC.

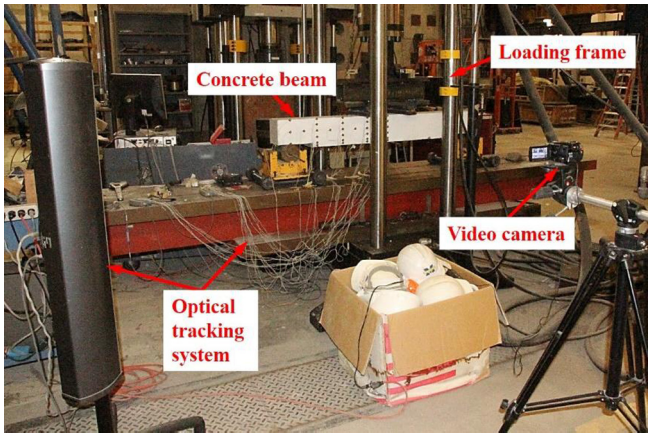

Fig. 6. Experimental setup and instrumentations of the four-point bending tests.

3.3. Load-displacement curves of the concrete beams

Four-point bending tests were conducted on the concrete beams with either CFRP-ECC hybrid strengthening or CFRP-mortar hybrid strengthening. The detailed experimental plan can be found in Section 2.3. The failure modes of all beams are presented in Fig. 11.

For the reference beam, it was observed that the flexural cracks firstly extended from the bottom and the beam finally failed by the concrete crushing on the top (Fig. 11a). As for the beam strengthened with the CFRP-mortar hybrid, the flexural cracks initially developed from the mortar layer and extended to the concrete beam. With the mortar layer cracking, the internal CFRP sheet was exposed bridging adjacent mortar blocks (Fig. 11b). When loaded further, due to the tensile load transferred from the CFRP sheet, the mortar layer either debonded from the concrete beam or cracked due to the same mechanism as shown in Fig. 10(b). The beam finally failed by concrete crushing on the top. As for the beam strengthened with the CFRP-ECC hybrid, the strengthening layer started pealing off from the concrete beam at both ends (Fig. 11c) when the load was around 15 kN. This debonding was also indicated in the load-displacement curve in Fig. 12 (see the circled region). With the increasing flexural load, the debonding horizontally extended from the end of the hybrid layer toward the mid-span of the beam. At the same time, flexural cracks were observed in the concrete beam. Due to debonding, the load could not be effectively transferred to the CFRP-ECC hybrid layer and therefore no cracking damage was observed in this layer. Finally, the beam failed by the concrete crushing on the top, similar to the other two beams. At the end of the four-point bending test, the CFRP-ECC layer almost detached from the concrete beam. The failure modes indicated that the interface between ECC and the concrete may become a problem when this CFRP-ECC hybrid is used for the strengthening of the concrete structures.

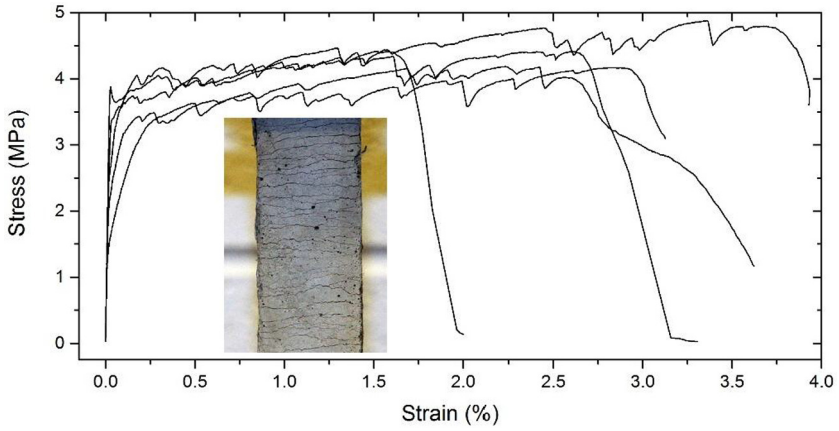

Fig. 7. Tensile stress-strain curves of ECC.

Table 5
Tensile properties of ECC and mortar.

Materials		First crack strength (MPa)	Tensile strength (MPa)	Tensile strain (%)
ECC	Mean	3.66	4.42	2.771
	SD	0.27	0.26	0.697
	COV	0.07	0.06	0.282
Mortar	Mean	NA	3.54	0.011
	SD	NA	0.34	0.002
	COV	NA	0.13	0.210

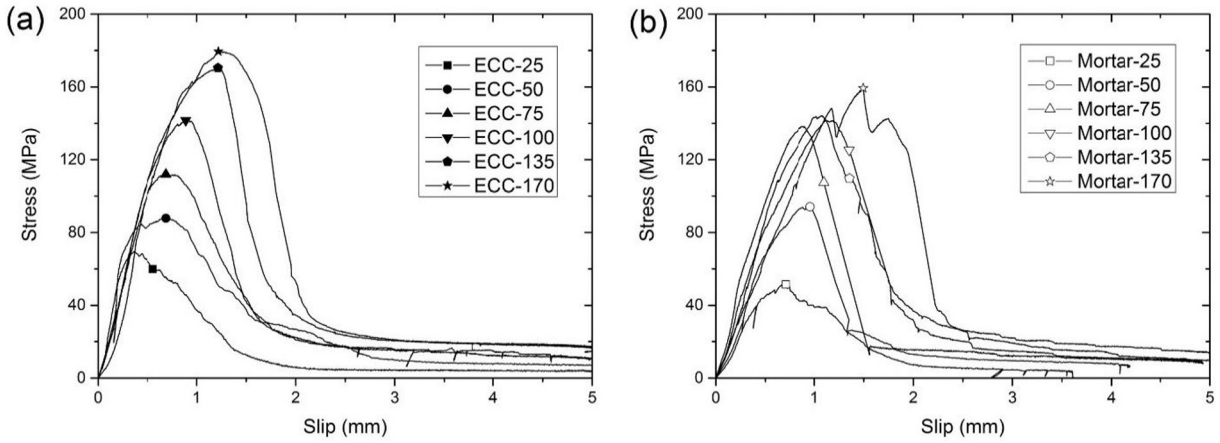

Fig. 8. Stress-slip curves of (a) ECC specimens and (b) mortar specimens.

The load-displacement curves of the three beams are plotted in Fig. 12. It can be seen that, the trends of the three load-displacement curves are very similar, with the load linearly increased with the displacement before a plateau was reached due to the yielding of the steel rebar. It can be seen in Fig. 12, the stiffness (slope of the linear stage) of the strengthened beams was higher than that of the reference beam (7.3×10^3 kN/m). This is mainly because of the increased cross section area after strengthening, i.e. the height of the beam increased from 152 mm (6 in) to 178 mm (7 in) with the strengthening layer. However, this increase in stiffness is marginal for CFRP-mortar hybrid (8.6×10^3 kN/m). This is because the mortar cracked very early under flexural loading and the integrity of the increased cross section was compromised (see Fig. 11b). It is obvious that the initial stiffness of the beam with CFRP-ECC hybrid is much higher than that of the reference beam, i.e. 25.5×10^3 kN/m, 2.5 times higher when the load was lower than 15 kN (see Fig. 12). Unfortunately, the CFRP-ECC hybrid strengthening layer started debonding at both ends in an early stage (see the circle notation in Fig. 12), and therefore the average stiffness of the beam decreased to 8.4×10^3 kN/m, which is similar to that of the CFRP-mortar strengthened beam. Since both strengthening systems experienced problems (i.e. cracking of mortar and debonding of ECC), they hardly contributed to the load carrying capacity of the concrete beam. For example, the ultimate load was 59.6 kN for the CFRP-mortar strengthened beam and 61.3 kN for the CFRP-ECC strengthened beam. They were very similar to the ultimate load of the reference beam, which was 60.3 kN.

3.4. Theoretical discussion on the strengthening potential of CFRP-ECC hybrid

It seems in Fig. 12 that both strengthening systems barely improved the flexural performance of the concrete beam. However,

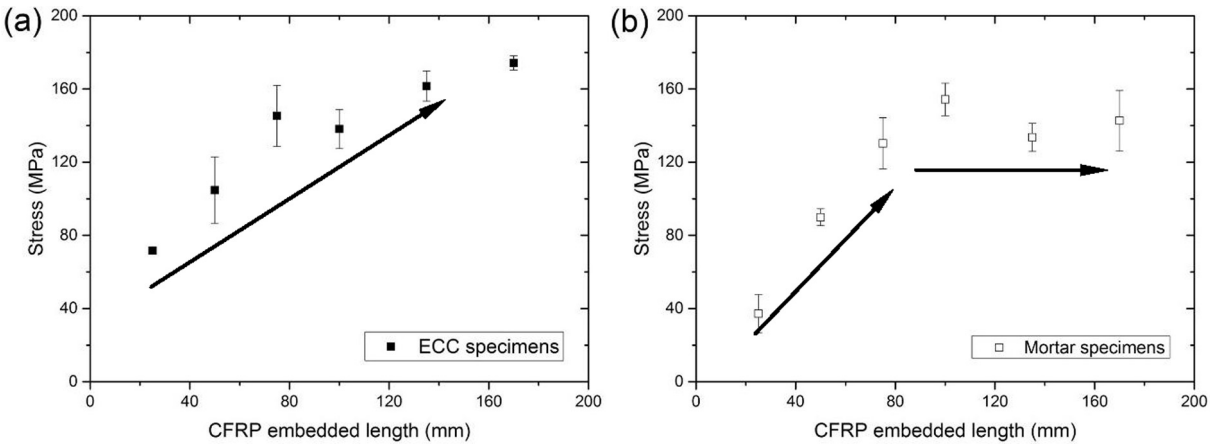

Fig. 9. Peak pull-out stress versus CFRP embedded length of (a) ECC specimens and (b) mortar specimens.

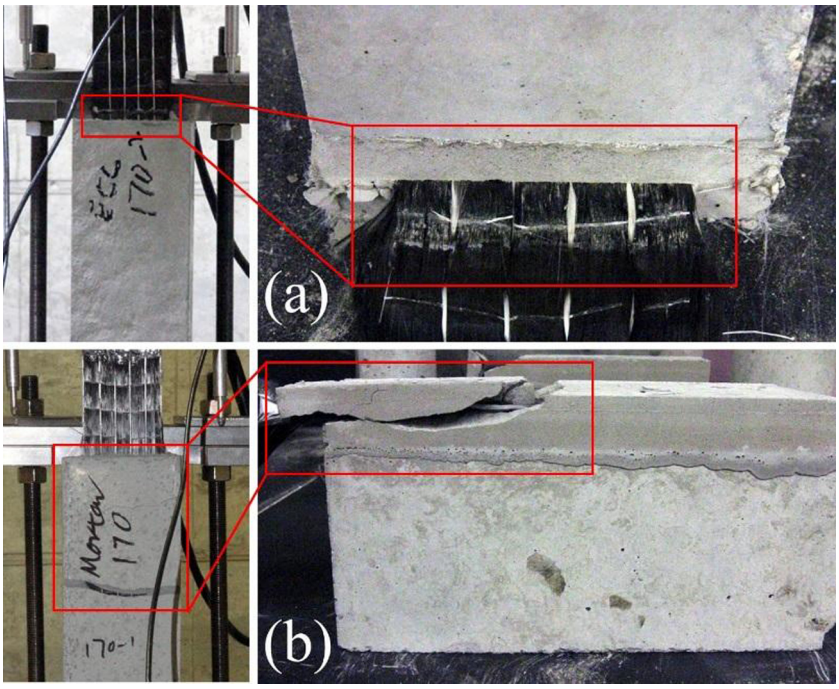

Fig. 10. Typical failure modes of (a) ECC specimen with CFRP pulled out and (b) mortar specimen with mortar shear cracking and CFRP pulled out from the rest of mortar matrix.

when carefully examined, the underlying mechanism which caused such reduced strengthening effect was totally different between the two strengthening systems. For ECC-mortar hybrid, the mortar was subjected to tensile cracking and fractured into a serious of mortar blocks. The blocks were connected by the internal CFRP sheet which was in tension. When the tensile load was transferred from CFRP sheet to the mortar, similar shear cracking occurred as observed in the pull-out tests (see Fig. 10b). Such a problem with CFRP-mortar hybrid strengthening system could not be solved without changing the material characteristics. This is also the reason why the mortar was replaced with ECC in the first place with desirable multi-cracking and strain hardening behaviors.

On the other hand, the strengthening effect of the CFRP-ECC hybrid was mainly limited by the debonding of the system from the concrete surface. The CFRP-ECC hybrid layer was carefully examined after being removed from the concrete beam. It was found that this hybrid layer was almost intact with no flexural cracks. This CFRP-ECC hybrid layer was also tested under the same four-point bending setup as the concrete beam. The load-displacement curve and the final failure mode are presented in Fig. 13. Though the hybrid layer was very thin (only 25 mm), the load still kept increasing with the displacement. This was attributed to the strain hardening behavior of ECC as well as the geometric nonlinear behavior of the hybrid. The CFRP-ECC hybrid layer showed extensive flexural curvature with a series of microcracks.

The results in Fig. 13 suggest that the strengthening potential of this CFRP-ECC hybrid can be realized as long as the interface debonding problem can be solved. Similar debonding issue was also encountered in [35], and a method to improve the interface between the CFRP-ECC hybrid and the concrete beam is proposed in Fig. 14. Instead of the surface treatment as in Fig. 6(a), the concrete beam can be prepared with the bottom surface mounted with a series of shear connectors.

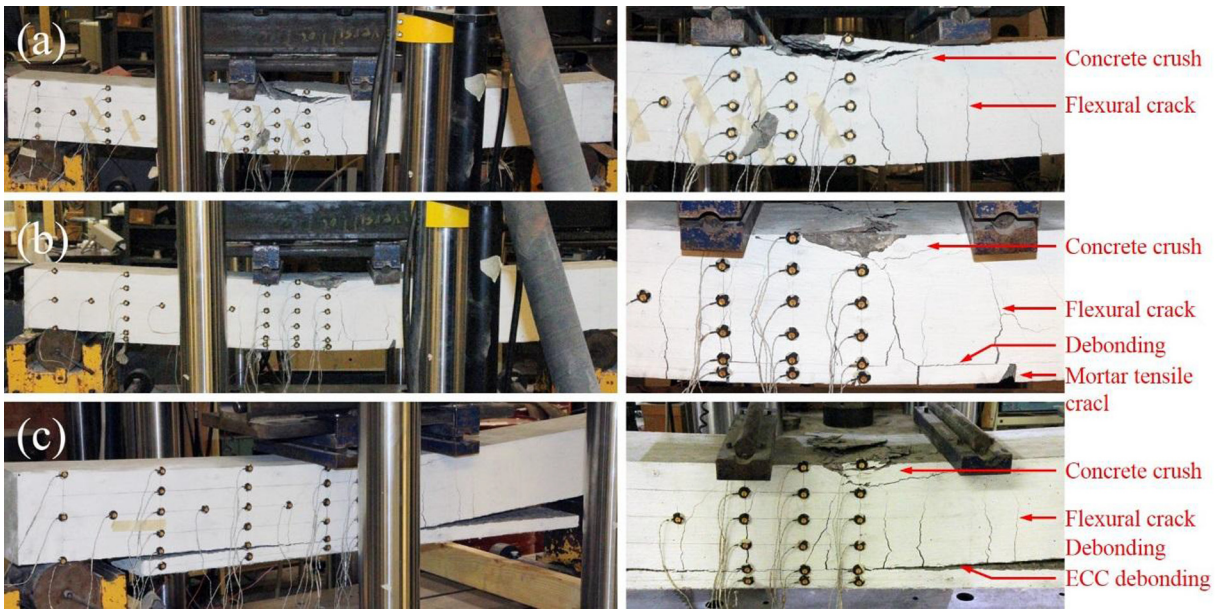

Fig. 11. Failure modes of concrete beams: (a) reference beam; (b) beam with CFRP-mortar hybrid strengthening and (c) beam with CFRP-ECC hybrid strengthening.

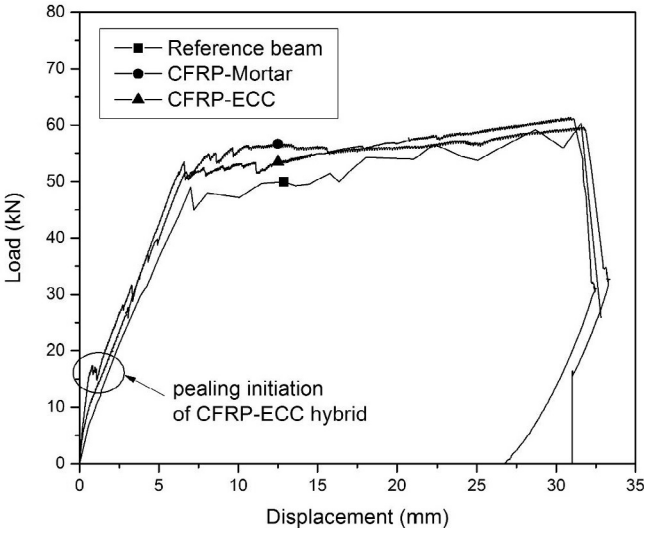

Fig. 12. Load-displacement curves of beams under four-point bending.

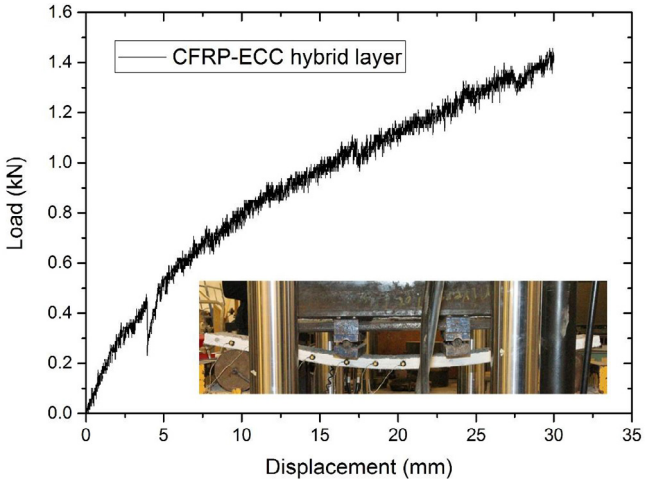

Fig. 13. Four-point bending of CFRP-ECC hybrid layer.

With the careful arrangement of the shear connectors, the debonding problem can be solved, and the CFRP-ECC hybrid can more effectively engage in the load carrying mechanism of the concrete beam. Then the question is how much improvement in the moment capacity of the concrete beam can be achieved, considering the contribution of the CFRP-ECC hybrid layer. The moment capacity of the beam with CFRP-ECC hybrid strengthening (M_{max}) can be expressed by the following equation:

$$M_{max} = M_{ref} + M_{hybrid} + P_{hybrid} \times \frac{h}{2} \tag{2}$$

$$M_{ref} = \frac{F_{ref}}{2} \times d \tag{3}$$

$$M_{hybrid} = \frac{F_{hybrid}}{2} \times d \tag{4}$$

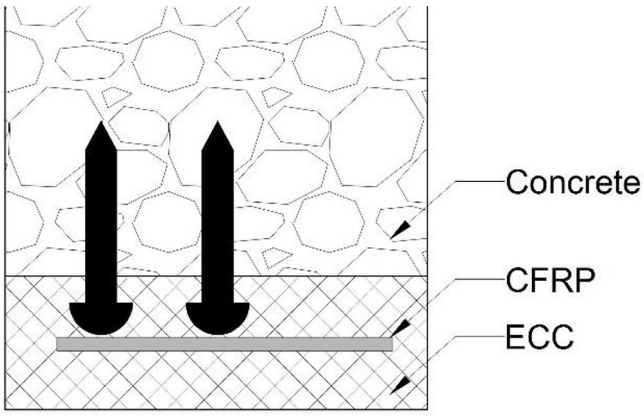

Fig. 14. Proposed method to prevent interface debonding between CFRP-ECC hybrid layer and concrete.

where M_{ref} is the moment capacity of the reference beam; M_{hybrid} is the corresponding moment capacity of the CFRP-ECC hybrid layer at the same displacement of the reference beam; P_{hybrid} is the pull-out force of the CFRP, and h (178 mm see Fig. 4) is the height of the strengthened beam. It is assumed that the neutral axis is at the middle of the strengthened section; d is the distance from the load to the closest support of the beam (d = 533 mm see Fig. 4).

F_{ref} can be found in Fig. 12 which is 60.3 kN with a corresponding displacement of 31.6 mm. In Fig. 13, F_{hybrid} is 1.4 kN corresponding to the same displacement as the reference beam. When calculating the pull-out force P_{hybrid}, it is assumed that the effective bond length of CFRP in ECC is 170 mm (see Fig. 9a), then P_{hybrid} is equal to the maximum pull-out stress 174.2 MPa multipled by the CFRP section area of 100×0.55 mm^2. Therefore P_{hybrid} is equal to 9.6 kN. According to the Eq. (2), the ultimate moment capacity of the concrete beam with the CFRP-ECC hybrid strengthening is 17.3 kN.m, showing a 7.6% increase comparing to the reference beam (16.1 kN.m using Eq. (3)).

It should be noted that, this calculated improvement in the moment capacity was based on the assumption that the effective bond length of CFRP in ECC was 170 mm. As can be seen in Fig. 9, the effective bond length can be longer and the pull-out stress may be higher than the value at 170 mm bond length. Therefore, this estimation (7.6%) is conservative. In addition, only one layer of 0.55 mm thick CFRP sheet was used in the current study. The moment capacity may be improved further when more layers of CFRP sheets are adopted. The moment capacity of the concrete beams with the CFRP-ECC hybrid and the shear coupler, and multiple layered CFRP, will be the subject of a future experimental investigation.

4. Conclusions

In the current study, a CFRP-ECC hybrid was proposed for the strengthening of the concrete structures. A comprehensive experimental program was conducted which consisted of three steps. Firstly, ECC with a strain capacity of 3% was developed and the compressive and tensile properties were calibrated. Then the interface between CFRP and ECC was investigated through the direct pull-out tests. Finally, concrete beams were prepared and strengthened with the CFRP-ECC hybrid. Four-point bending tests were carried out to study the performance of the strengthening system. Based on the results in this paper, it could be concluded that:

(a) The tensile strain capacity of ECC in the current paper was tested as 2.8% (average), which was almost 252 times higher than that of the cement mortar.
(b) In terms of the interface behavior, for the CFRP-ECC hybrid, the peak pull-out stress was proportional to the CFRP embedded length. The peak stress increased from 71.6 MPa to 174.2 MPa when the embedded length increased from 25 mm to 170 mm. On the other hand, as for the CFRP-mortar hybrid, the peak pull-out stress stopped increasing when the embedded length exceeded 100 mm. With 25 mm embedded length, the pull-out stress was 37.2 MPa. After 100 mm, the pull-out stress became constant in the range of 133.5 MPa–154.3 MPa.
(c) Through the pull-out tests, it was found that, the effective bond length of CFRP in ECC was longer than 170 mm. As for mortar, the effective bond length of CFRP was in the range of 100 mm–135 mm.
(d) In the four-point bending tests of the concrete beams, it was found that the CFRP-mortar hybrid failed by the brittle cracking and debonding from the concrete beam. On the other hand, the CFRP-ECC hybrid started pealing off from the concrete beam at an early stage. Due to these premature failure mechanisms, the flexural behavior of the concrete beam was barely improved by either hybrid system.
(e) Theoretical analysis indicated that, the moment capacity of the concrete beam with the CFRP-ECC hybrid strengthening could increase by more than 7.6%, if the interface between ECC and concrete could be secured.

From the theoretical analysis and the flexural testing of the CFRP-ECC hybrid alone (see Fig. 13), CFRP-ECC hybrid exhibited a good potential for the strengthening of the concrete structures. This paper pointed out for the first time the interface issue between ECC and concrete, which provides precautions for the future application of this hybrid for the strengthening of the concrete structures. The results indicated that the direct casting of the fresh ECC to the concrete surface was not sufficient to ensure the bonding of the two, even though the surface of the concrete was prepared with surface treatments beforehand. Therefore, it was highly recommended that shear keys be designed and installed on the concrete surface before attaching the CFRP-ECC hybrid layer. This would effectively secure the bond of ECC and concrete for not only room temperature applications, but also for conditions concerning elevated temperatures. Other techniques existing in the literature to postpone or totally prevent debonding of FRP sheets from concrete substrate, i.e. grooving method (GM) governed through EBROG [45,46] and EBRIG [47] techniques, can also be borrowed and tested for the CFRP-ECC hybrid for the strengthening of the concrete beams.

It is recommended that more four-point bending tests should be conducted to generate useful information on the FRP-ECC hybrid for the beam strengthening. Unfortunately, this could be only possible when the issue of the interface debonding between the CFRP-ECC hybrid and the concrete can be solved. This can be achieved by focusing the next stage research on the interface treatment methods, such as grooving method (GM) governed through EBROG and EBRIG techniques. After existing interface treatment methods were proved, or other innovative interface treatment methods were developed, can the CFRP-ECC hybrid be used for the strengthening of the concrete beams.

Acknowledgments

The authors gratefully acknowledge the financial support provided by the Australian Ministry of Education through the Endeavour Research Fellowship scheme (BR14-003378/44882015) and the Thousand Talents Plan (Young Professionals) in China through the Fundamental Research Funds for the Central Universities (YWF-16-RSC-013). This work was also partially funded by the National Science foundation of China (51608020). Dr. Sukmin Kwon and Mr. Motohiro Ohno are acknowledged for their assistance with the experimental tests.

References

[1] Teng JG, Chen JF, Smith ST, Lam L. FRP Strengthened RC Structures. West Sussex, UK: John Wiley and Sons Ltd; 2002.
[2] Chen Y, Davalos J, Ray I, Kim HY. Accelerated aging tests for evaluations of durability performance of FRP reinforcing bars for concrete structures. Compos Struct 2007;78(1):101–11.
[3] Abdalla JA, Harib F, Hawileh R, Mirghani A. Experimental investigation of bond slip behavior of aluminum plates adhesively bonded to concrete. J Adhes Sci Technol 2016;30(25):82–99.
[4] Ali AL, Abdalla JA, Hawileh R, Galal K. CFRP mechanical anchorage for externally strengthened RC beams under flexure. Phys Procedia 2014;55:10–6.
[5] Larbi AS, Agbossou A, Hamelin P. Experimental and numerical investigations about textile-reinforced concrete and hybrid solutions for repairing and/or strengthening reinforced concrete beams. Compos Struct 2013;99:152–62.

[6] Michels J, Czaderski C, El-Hacha R, Brönnimann R, Motavalli M. Temporary bond strength of partly cured epoxy adhesive for anchoring prestressed CFRP strips on concrete. Compos Struct 2012;94(9):2667–76.
[7] Hawileh R, Rasheed H, Abdalla JA, Tamimi A. Behavior of reinforced concrete beams strengthened with externally bonded hybrid fiber reinforced polymer systems. Mater Des 2014;53:972–82.
[8] Hollaway LC, Leeming MB. Strengthening of Reinforced Concrete Structures: Using Externally-bonded FRP Composites in Structural and Civil Engineering. Cambridge, UK: Woodhead Publishing; 1999.
[9] Naser M, Hawileh R, Abdalla JA, Al Tamimi A. Bond behavior of CFRP cured laminates: experimental and numerical investigation. J Eng Mater Technol 2012;134(2). 021002.1021002.9.
[10] Kalfat R, Al-Mahaidi R. Development of a hybrid anchor to improve the bond performance of multiple plies of FRP laminates bonded to concrete. Constr Build Mater 2015;94:280–9.
[11] Tamimi A, Hawileh R, Abdalla JA, Rasheed H. Effects of ratio of CFRP plate length to shear span and end anchorage on flexural behavior of SCC R/C Beams. J Compos Constr 2011;15(6):908–19.
[12] Gamage J, Al-Mahaidi R, Wong MB. Bond characteristics of CFRP plated concrete members under elevated temperatures. Compos Struct 2006;75 (1):199–205.
[13] Michels J, Widmann R, Czaderski C, Allahvirdizadeh R, Motavalli M. Glass transition evaluation of commercially available epoxy resins used for civil engineering applications. Compos B Eng 2015;77:484–93.
[14] Dong K, Hu K. Development of bond strength model for CFRP-to-concrete joints at high temperatures. Compos B Eng 2016;95:264–71.
[15] Bai Y, Keller T. Effects of thermal loading history on structural adhesive modulus across glass transition. Constr Build Mater 2011;25(4):2162–8.
[16] Al-Safy R, Al-Mahaidi R, Simon GP. A study of the use of high functionality-based resin for bonding between CFRP and concrete under harsh environmental conditions. Compos Struct 2013;95(1):295–306.
[17] Gamage K, Al-Mahaidi R, Wong B. FE modelling of CFRP-concrete interface subjected to cyclic temperature, humidity and mechanical stress. Compos Struct 2010;92(4):826–34.
[18] Moussa O, Vassilopoulos AP, Keller T. Experimental DSC-based method to determine glass transition temperature during curing of structural adhesives. Constr Build Mater 2012;28(1):263–8.
[19] Petkova D, Donchev T, Wen J. Experimental study of the performance of CFRP strengthened small scale beams after heating to high temperatures. Constr Build Mater 2014;68:55–61.
[20] López C, Firmo JP, Correia JR, Tiago C. Fire protection systems for reinforced concrete slabs strengthened with CFRP laminates. Constr Build Mater 2013;47:324–33.
[21] Hashemi S, Al-Mahaidi R. Flexural performance of CFRP textile-retrofitted RC beams using cement-based adhesives at high temperature. Constr Build Mater 2012;28(1):791–7.
[22] Hashemi S, Al-Mahaidi R. Experimental and finite element analysis of flexural behavior of FRP-strengthened RC beams using cement-based adhesives. Constr Build Mater 2012;26(1):268–73.
[23] Tetta ZC, Koutas LN, Bournas DA. Shear strengthening of full-scale RC T-beams using textile-reinforced mortar and textile-based anchors. Compos B Eng 2016;95:225–39.
[24] D'Ambrisi A, Focacci F. Flexural strengthening of RC beams with cement-based composites. J Compos Constr 2011;15(5):707–20.
[25] Elsanadedy HM, Almusallam TH, Alsayed SH, Al-Salloum YA. Flexural strengthening of RC beams using textile reinforced mortar-experimental and numerical study. Compos Struct 2013;97:40–55.
[26] Triantafillou TC, Papanicolaou CG. Shear strengthening of reinforced concrete members with textile reinforced mortar (TRM) jackets. Mater Struct 2006;39 (285):93–103.
[27] Tzoura E, Triantafillou TC. Shear strengthening of reinforced concrete T-beams under cyclic loading with TRM or FRP jackets. Mater Struct 2016;49(1):17–28.
[28] Li VC. On engineered cementitious composites (ECC). J Adv Concr Technol 2003;1(3):215–30.
[29] Maalej M, Leong KS. Engineered cementitious composites for effective FRP-strengthening of RC beams. Compos Sci Technol 2005;65(7–8):1120–8.
[30] Li VC. Tailoring ECC for special attributes: a review. Int J Concr Struct Mater 2012;6(3):135–44.
[31] Şahmaran M, Li VC. Durability of mechanically loaded engineered cementitious composites under highly alkaline environments. Cem Concr Compos 2008;30(2):72–81.
[32] Yu JT, Lin JH, Zhang ZG, Li VC. Mechanical performance of ECC with high-volume fly ash after sub-elevated temperatures. Constr Build Mater 2015;99:82–9.
[33] Zheng YZ, Wang WW, Brigham JC. Flexural behaviour of reinforced concrete beams strengthened with a composite reinforcement layer: BFRP grid and ECC. Constr Build Mater 2016;115:424–37.
[34] Dai JG, Wang B, Xu SL. Textile reinforced engineered cementitious composites (TR-ECC) overlays for the strengthening of RC beams. In: Proceedings of the Second Asia-Pacific Conference on Fiber Reinforced Polymers in Structures. Seoul, Korea; 2009.
[35] Wu C, Li VC. Thermal-mechanical behaviors of CFRP-ECC hybrid under elevated temperatures. Compos B Eng 2016. http://dx.doi.org/10.1016/j.compositesb.2016.11.037.
[38] ASTM C190/C190M-16a. Standard Test Method for Compressive Strength of Hydraulic Cement Mortars (using 2-in. or [50-mm] Cube Specimens). West Conshohocken, PA: ASTM International; 2016.
[39] Felekoglu B, Tosun-Felekoglu K, Ranade R, Zhang Q, Li VC. Influence of matrix flowability, fiber mixing procedure, and curing conditions on the mechanical performance of HTPP-ECC. Compos B Eng 2014;60:359–70.
[40] JSCE. Recommendations for Design and Construction of High Performance Fiber Reinforced Cement Composites with Multiple Fine Cracks. Tokyo: Japan Society of Civil Engineers; 2008.
[41] ASTM D3039-14. Standard Test Method for Tensile Properties of Polymer Matrix Composite Materials. West Conshohocken, PA: ASTM International; 2014.
[42] ASTM C873/C873M. Standard Test Method for Compressive Strength of Concrete Cylinders Cast in Place in Cylindrical Molds. West Conshohocken, PA: ASTM International; 2015.
[43] ASTM A615/A615M-16. Standard Specification for Deformed and Plain Carbon-Steel Bars for Concrete Reinforcement. West Conshohocken, PA: ASTM International; 2015.
[44] Hosseini A, Mostofinejad D. Effective bond length of FRP-to-concrete adhesively-bonded joints: experimental evaluation of existing models. Int J Adhes Adhes 2014;48:150–8.
[45] Hosseini A, Mostofinejad D. Effect of groove characteristics on CFRP-to-concrete bond behavior of EBROG joints: experimental study using particle image velocimetry (PIV). Constr Build Mater 2013;49:364–73.
[46] Mostofinejad D, Tabatabaei Kashani A. Experimental study on effect of EBR and EBROG methods on debonding of FRP sheets used for shear strengthening of RC beams. Compos B Eng 2013;45(1):1704–13.
[47] Mostofinejad D, Shameli SM. Externally bonded reinforcement in grooves (EBRIG) technique to postpone debonding of FRP sheets in strengthened concrete beams. Constr Build Mater 2013;38:751–8.